Lab 2 for benzene

Andriy Zhugayevych

October 29, 2020

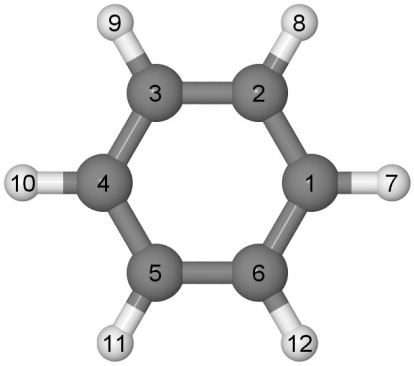

Figure 1: The molecule under the study.

The molecule under the study is benzene, chemical formula C_6H_6, see Fig. 1. We use (TD)DFT with B3LYP density functional [1] combined with 6-31G* basis set. Solvent effects are modeled by PCM implicit solvation model [2]. All calculations are performed in Gaussian 16 program [3]. For symmetry analysis we use Bilbao Crystallographic Server [4]. Also, when discussing molecular geometries in a lowered symmetry we assume the coordinate system to be oriented as in Fig. 1, in particular, bond lengths C_1C_2 and C_1C_6 are equal in mmm symmetry.

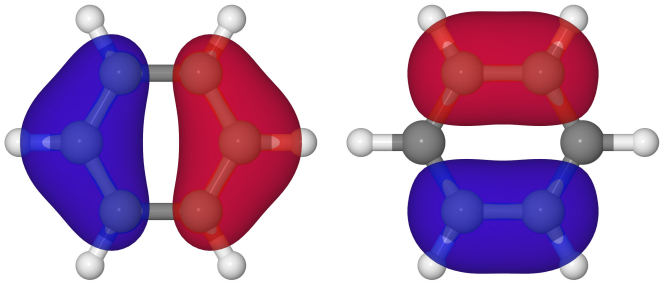

Figure 2: Doubly degenerate HOMO at -6.70 eV.

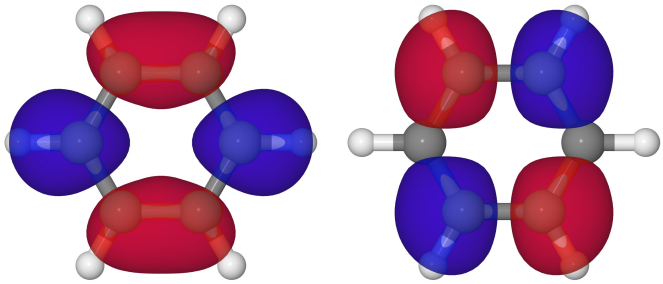

Figure 3: Doubly degenerate LUMO at +0.10 eV.

Table 1: Summary of the energy gaps.

	E(eV)
HOMO-LUMO	6.80
IP-EA	6.71
excited singlet (S_1)	5.54
relaxed S_1	5.27
relaxed triplet (T_1)	3.88

Table 2: Summary of the geometries and solvation energies. Here ΔCC is the average CC bond length relative to the ground state for which CC=1.397 Å, BLA is the bond length alternation which is the half-difference between C_2C_3 and C_1C_2 bond lengths.

state	sym.	ΔCC(Å)	BLA(Å)	$E_{\rm solv}$(eV)
ground state	6/mmm	0	0	0.073
cation	mmm	.016	−.030	2.216
anion	mmm	.023	+.033	2.437
excited singlet	6/mmm	.031	0	0.072
triplet	mmm	.037	+.066	0.066

The ground state molecular geometry is shown in Fig. 1 [molec_B3LYPp2p_em]. There are no other conformers. The molecule is planar with the symmetry 6/mmm. The length of all CC bonds is 1.40 Å indicative for a delocalized (aromatic) π-conjugated system. The frontier orbitals are doubly degenerate HOMO and LUMO shown in Figs. 2 and 3 [molec_B3LYPp2p_mo]. Their symmetries are e_{1g} and e_{2u} respectively. The HOMO-LUMO gap is given in Table 1 together with other energy gaps.

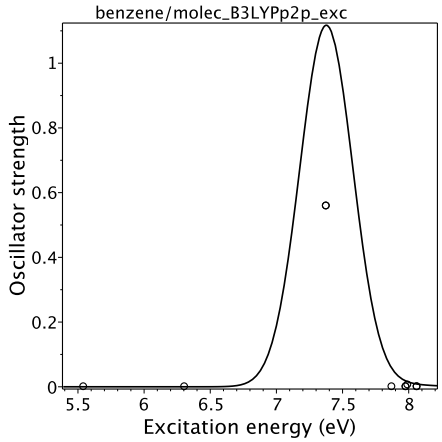

Figure 4: Electronic excitations.

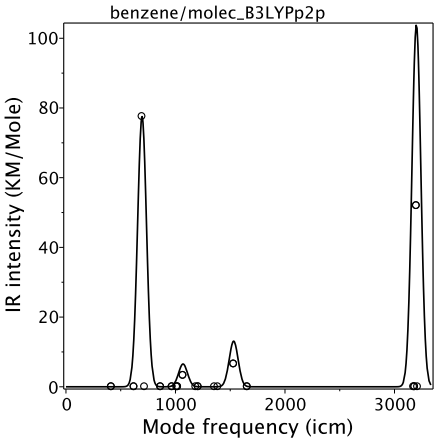

Figure 5: IR spectrum.

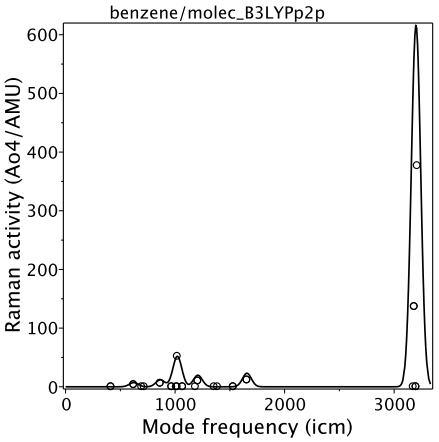

Figure 6: Raman activities.

The calculated low-energy UV-Vis absorption spectrum [molec_B3LYPp2p_exc] (see the transition spectral density in Fig. 4) contains only one dipole-allowed excitation corresponding to doubly degenerate HOMO-LUMO ($\pi - \pi^*$) transition at 7.4 eV ($S_{3,4}$ of E_{2u} symmetry) with the oscillator strength of 0.56 per transition. The states S_1 (B_{2u}) and S_2 (B_{1u}) are dark in the Franck–Condon approximation but should be observable through the Herzberg–Teller effect [5]. All the four lowest excited states correspond to HOMO-LUMO transition (decomposition $e_{1g} \times e_{2u} = b_{1u} + b_{2u} + e_{1u}$) as confirmed by NTO analysis [molec_B3LYPp2p_nto*]. For benzene molecule Rydberg states should be taken into account [6] that requires larger basis sets and is beyond the scope of this work.

Because the S_1 state is dark (dipole-forbidden transition) the fluorescence is weak. Formally the Stokes shift is 0.3 eV [molec_R_B3LYPp2p_em/exc] (see Table 1) and the emission lifetime is infinite — the formula is as follows:

$$\tau = \frac{1}{2\alpha^3 n_{\mathrm{refrac}} f_{\mathrm{osc}}} \frac{m_{\mathrm{e}} e^4}{\hbar E^2}.$$

In the relaxed triplet state (T_1) the 6/mmm symmetry is lowered to mmm, and strong BLA pattern appears with long C_2C_3 bond and short C_1C_2 and C_3C_4 bonds, see Table 2 [molec_T_B3LYPp2p_em]. NO analysis [molec_T_B3LYPp2p_no] shows that the triplet is a single electron HOMO-LUMO excitation between the MOs shown on the right sides of Figs. 2 and 3. The resulting depletion of the electronic density on bonds C_2C_3 and C_5C_6 explains the observed BLA pattern. The vertical T_1 energy calculated by ΔSCF [molec_T_B3LYPp2p_sp/0] is given in Table 1, the TDDFT value is 2.96 eV [molec_T_B3LYPp2p_excT].

The calculated vertical IP and EA are 9.01 eV and -2.30 eV respectively [molec_B3LYPp2p_P/N]. The geometry relaxation (polaron) effects change IP/EA by 0.15/0.20 eV [molec_P/N_B3LYPp2p_em/sp]. NO analysis [molec_P/N_B3LYPp2p_no] shows that the hole orbital of the cation is the HOMO shown on the left side of Fig. 2, and the depletion of electronic density on this MO explains the BLA pattern in Table 2. For the anion, the extra electron goes into the LUMO shown on the right side of Fig. 3 increasing electronic density on bonds 12, 16, 34, 45 thus resulting in the opposite BLA pattern. Interestingly, the BLA pattern of cation is different from that of anion and triplet. For all the three states, the geometry with the opposite BLA pattern is a saddle point descending to the correct BLA pattern via imaginary frequency mode B_{3g} (mmm point group) [molec-x*].

Solvation energies of different states in water are given in Table 2 [molec_wat*_B3LYPp2p_em/sp/exc]. As expected the only large numbers are observed for ions resulting in dramatic changes of IP/EA, whereas the changes in the gap energies are negligible except for IP-EA gap which increases by 0.3 eV. Note that tight optimization of S_1 state in water is not converging due to numerical errors but analysis of the optimization dynamics and frequencies confirm that the obtained geometry is well relaxed [molec_wat_R_B3LYPp2p_emcheck/freq].

IR/Raman spectra are given in Figs. 5 and 6 [molec_B3LYPp2p_freq*]. The strongest IR-active transitions correspond to vibrational modes A_{2u} at 695 cm^{-1} [#5] and E_{1u} at 3200 cm^{-1} [#28-29] representing three orthogonal displacements of hydrogens relative to carbons (z for A_{2u} and x, y for E_{1u}). The strongest Raman-active transitions also correspond to CH stretching and include modes A_{1g} (z^2 symmetry) at 3211 cm^{-1} [#30] and E_{2g} ($xy, x^2 - z^2$ symmetry) at 3184 cm^{-1} [#26-27]. The next strongest transitions correspond to CC stretching and include modes A_{1g} at 1021 cm^{-1} [#13] and E_{2g} at 1656 cm^{-1} [#23-24]. The full-symmetry mode

[#13] is the mode with the largest vibronic coupling to HOMO-LUMO excitations (Huang–Rhys factor $\gtrsim 1$ for S_1-S_4). The weaker Raman-active modes correspond to CH bending, CH torsion (E_{1g} or xz, yz symmetry), and CCC bending.

Table 3: Comparison of calculations performed in this work ("this" column) with experimental data ("exp') and best available calculations ("ref"). For geometry, vibrations, and ground state energies the reference method is CCSD(T)/cc-pVTZ (for EA aug-cc-pVTZ basis set gives -0.55 eV [10]). For singlet excitations the reference method is STEOM-CCSD [12]. For triplets the reference is CASSCF(6,12)/cc-pVTZ [11].

	exp	this	ref
Bond length (Å) [8]			
CC	1.397	1.397	1.398
CH	1.084	1.087	1.083
Vibrational frequency (cm^{-1}) [7]			
IR A_{2u}	673	695	686
IR E_{1u}	3063	3200	3198
Raman A_{1g}	3062	3211	3209
Raman E_{2g}	3047	3184	3181
Raman A_{1g}	992	1021	1005
Raman E_{2g}	1596	1656	1637

	exp	this	ref
Energy (eV) [9, 10]			
IP	9.24	9.01	9.36
EA		-2.30	-1.99
Excitation energy (eV) [11, 12, 6]			
singlet B_{2u}	4.90	5.54	4.81
singlet B_{1u}	6.20	6.31	6.47
singlet E_{1u}	6.94	7.38	7.15
triplet B_{1u}	3.95	3.80	3.85
triplet E_{1u}	4.76	4.79	4.83
triplet B_{2u}	5.60	5.21	6.78
triplet E_{2g}	6.83	7.43	7.15

Supporting Information

Attached are output and xyz files, the notations are as follows. States: "P" = cation, "N" = anion, "T" = triplet, "R" = excited singlet S1, "S2" = excited singlet S2, "O" = neutral ground state, if two such symbols are present the first determines the geometry and the second corresponds to the single point calculations. Methods: "p2p" = 6-31G*, "c3" = cc-pVTZ, "c3a" = aug-cc-pVTZ. Solvents: "wat" = water. Types of calculations: "em" = energy minimization, "sp" = single point, "freq" = vibrational frequencies, "exc" = excited singlets, "excT" = excited triplets, "mo" = molecular orbitals, "no" = natural orbitals, "nto" = natural transition orbitals.

References

[1] A D Becke, J Chem Phys 98, 5648 (1993); P J Stephens, F J Devlin, C F Chabalowski, M J Frisch, J Phys Chem 98, 11623 (1994)

[2] J Tomasi, B Mennucci, R Cammi, Chem Rev 105, 2999 (2005)

[3] M J Frisch et al, Gaussian 16, Revision B.01, Gaussian, Inc., Wallingford CT, 2016

[4] http://www.cryst.ehu.es/cgi-bin/rep/programs/sam/point.py?sg=191&num=27

[5] J Li, C Lin, X Li, C Zhu, S Lin, Phys Chem Chem Phys 12, 14967 (2010)

[6] Y Li, J Wan, X Xu, J Comp Chem 28, 1658 (2007)

[7] NIST Chemistry WebBook,https://webbook.nist.gov

[8] NIST Computational Chemistry Comparison and Benchmark DataBase, http://cccbdb.nist.gov

[9] M S Deleuze, L Claes, E S Kryachko, J P Francois, Benchmark theoretical study of the ionization threshold of benzene and oligoacenes, JCP 119, 3106 (2003)

[10] B Hajgato, M S Deleuze, D J Tozer, F De Proft, J Chem Phys 129, 084308 (2008)

[11] T Hashimoto, H Nakano, K Hirao, J Chem Phys 104, 6244 (1996)

[12] M Nooijen, Spectrochimica Acta Part A 55, 539 (1999)